

Interference Methods In The Testing And Fabrication Of New- Design Grazing Incidence Gratings

Michael C. Hettrick and Christopher Martin

Proc. Soc. Photo-Opt. Instr. Eng. vol. 503, pp. 106-113 (1984)

<http://dx.doi.org/10.1117/12.944820>

Copyright 1984 Society of Photo Optical Instrumentation Engineers. One print or electronic copy may be made for personal use only. Systematic electronic or print reproduction and distribution, duplication of any material in this paper for a fee or for commercial purposes, or modification of the content of the paper are prohibited.

Interference Methods in the Testing and Fabrication of New-Design Grazing Incidence Gratings

Michael C. Hettrick and Christopher Martin

University of California, Space Sciences Laboratory, Berkeley, CA 94720

Abstract

Recent work in the design of soft X-ray and extreme UV spectrographs has identified a new class of reflection gratings whose aberrations do not increase at grazing incidence. To achieve this characteristic, the groove spacings are varied in a continuous manner across a plano grating aperture. Ray traces of the concentric groove grating, the oriental fan grating and variations illustrate their potential for space astronomy and laboratory applications in the wavelength range of approximately $\lambda \sim 10-1000 \text{ \AA}$. Both straight-groove and concentric-groove patterns have been successfully fabricated with varied line spacings through mechanical ruling techniques. A concave varied line-space grating has been measured to achieve 70% of its theoretical efficiency in the extreme UV. An interferometric method of fabrication is also discussed, in which the recording wavelength is scaled-up into the far UV or even visible region of the spectrum. This holographic grating is designated "Type V." Two interferometers capable of recording grating wavefront aberrations in the extreme UV and soft X-ray are proposed.

Introduction

Spectroscopic study of astronomical sources is the most powerful tool available to the astrophysicist. This is especially important in the soft X-ray ($\lambda \sim 10-100 \text{ \AA}$) and in the extreme UV ($\lambda \sim 100-1000 \text{ \AA}$), where the absence of suitable instrumentation is in part responsible for the paucity of data available at these wavelengths. This has obstructed our understanding of the physical processes occurring in many interesting and energetic astronomical objects (e.g., quasars, X-ray binaries, cataclysmic variables and white dwarfs).^{1,2}

Recently, we have proposed several new solutions for the design of reflection grating spectrometers.³⁻⁵ Figure 1 is a schematic illustration of the unusual grating geometries employed in such spectrometers. Unique features of these gratings are: (1) illumination of a plano grating by converging light, (2) a large variation ($\sim 100\%$) in the groove spacings across the aperture, and (3) a simultaneous minimization, at grazing incidence, of spectral and spatial imaging aberrations. In comparison to conventional spectrometers operating in the soft X-ray and extreme UV (EUV), these new systems are calculated to yield performance increases of one to two orders of magnitude in spectral resolution and approximately one order of magnitude in efficiency.

In this paper, we report on initial progress which has been made in the practical development of these proposed gratings. We discuss ongoing work which is relevant to their successful implementation in a space-borne flight spectrometer and a laboratory spectrometer, and address methods of fabrication and testing employing interferometry. First, however, we review the performance capabilities which have motivated the design and construction of these varied line-space grating spectrometers.

Performance Characteristics of New Spectrometers

The performance of a grating spectrometer can be largely summarized in terms of three principal criteria: (1) resolution, (2) efficiency, and (3) stray light. In this section, we briefly discuss the advantages realized by the proposed grating designs in all three areas.

Resolution

A striking property of this grating class is that the grating aberrations do not worsen towards grazing incidence. In fact, minimum grating aberrations are achieved in the limit of a vanishingly small graze angle. However, given aberrations which inevitably precede the grating, such as those inherent in the collecting optics, a larger graze angle of reflection is favored on the basis of the increased dispersive power. However, these graze angles are small in comparison to the required normal incidence mountings for conventional gratings having similar resolution (e.g., a concave Rowland circle grating).

If situated in converging light, a conventional plano grating will suffer from extreme astigmatic and comatic aberrations.⁶ The smoothly varying groove spacings of the proposed designs largely, or completely, overcomes this effect. Two distinct levels of aberration-

correction are possible:

(1) Straight grooves in an otherwise classical in-plane geometry (Figure 1a) or in a (conical) off-plane fan geometry (Figure 1b) completely remove astigmatism and the dominant term in coma. In typical astronomical mountings, using light converging at a speed of f5-f10, spectral resolutions of $\lambda/\Delta\lambda \sim \text{few} \times 10^2$ are attained. Figure 2a is the result of ray trace calculations⁴ for an in-plan straight groove solution using an f6 beam, reveals that such resolution extends over a wide instantaneous band. In a laboratory instrument, where slower beams (e.g., f30) are more common, resolutions near 10^4 are attainable with these designs.

(2) Additional spatial variations in the groove spacings permit higher-order corrections to be applied. For example, stigmatic imaging is provided by the curved (e.g., concentric) grooves shown in Figure 1c. Figures 2b and 2d confirm this, and reveal excellent imaging over a finite spectral band near the stigmatically-corrected wavelength at $\lambda 304 \text{ \AA}$. Further, quasi-stigmatism is available through use of a fan groove pattern whose angular spacings increase at towards the edges of the fan.⁴ Thus, both in-plane and off-plane gratings are found to exhibit the ability to attain $\lambda/\Delta\lambda = \text{several} \times 10^4$ over useable bandpasses.

The varied-angle fan grating is the ideal candidate for use as an echelle fed by a concentric groove pre-disperser. Figure 3 is an illustration of a promising instrument design for space astronomy, utilizing a new class of collecting mirror telescope.⁵ Ray traces of the grating system reveal a resolution of 30,000 over a 30% range in wavelength, as shown in Figure 4. This grazing incidence design can extend to approximately $\lambda 100 \text{ \AA}$ at this resolution. Detailed calculations which elaborate upon this result will be reported in future publications.

Efficiency

In contrast to conventional high-resolution spectrometers, the proposed designs operate without additional optics (e.g., collimators, relay optics or camera mirrors). A minimum number of reflections is thereby achieved, all at grazing incidence. The resulting efficiencies which can be attained are therefore extremely high. For example, a single grating at a 10° graze angle (approximately 40% absolute efficiency in the EUV) results in a telescope/grating/detector instrument which operates at a net efficiency of 5% relative to the geometric telescope aperture. In an echelle mode (Figure 3), a net efficiency of approximately 1.5% is expected.⁵

Varied groove spacings on a concave grating have been mechanically ruled and used in a laboratory grazing incidence spectrometer by Kita et al.⁷ Measurements of its efficiency in the EUV have recovered 65-70% of the theoretical values.⁸ Thus, varied spacings can be ruled with a high groove efficiency as conventional gratings.

Stray Light

We have found a low level of stray or scattered light in the EUV for the concave grating discussed above.⁸ A continuum level of only $10^{-5}/\text{\AA}$ was measured in first order at a wavelength pixel 50 \AA away from the parent line at $\lambda 304 \text{ \AA}$. The profile of this scattered light was similar to that of the zero order distribution, suggesting that groove location errors were not the dominant contribution. This initial measurement is in agreement with the theoretical expectation that groove misplacements must be small when ruled with an engine which has been upgraded to permit accurate and independent positioning of grooves. In addition, light scattered from periodic ruling errors should not give rise to Rowland ghosts (as in a conventional grating), since the ratio of the periodic error to the (varied) groove spacings is not in resonance. Thus, there are several straightforward reasons to expect the level of stray light to be consistently low for a varied line-space grating.

Proto-type Grating Fabrication and Testing

A straight-groove varied line-space plano grating (Figure 1a) has been mechanically ruled by Hitachi Instruments Inc. as part of the pre-flight effort in support of the Extreme Ultraviolet Explorer satellite.⁹ Electron micrographs of the Hitachi grating appear in Figure 5. This grating is currently being tested in the EUV, using the apparatus illustrated in Figure 6. The grating is situated in a converging beam representative of that provided in the actual flight instrument. The functional imaging properties of the grating are therefore manifested in the spot sizes produced at the detector. Such an optical system therefore also constitutes a laboratory spectrometer, which can be used to study the properties of sources emitting in the EUV. At wavelengths above approximately $\lambda 304 \text{ \AA}$, the small normal incidence optic can be coated in a conventional manner (e.g., with Osmium). Such a mirror is also being coated with Mo/Si multi-layers to permit coverage to wavelengths as short as 130 \AA . Near-normal incidence reflectances of Mo/Si mirrors have been measured at greater than 50%.¹⁰ This apparatus should provide an efficient means of measuring grating resolution and stray light profile.

Concentric-groove gratings with varied spacings have been mechanically ruled through an in-house effort at the Perking-Elmer Corporation.¹¹ We expect that such technology can be extended to include the design geometries relevant to grazing incidence use. It is interesting to recall that Sakayanagi¹² both designed and ruled a concentric groove concave grating (the "circular groove grating") thirty years ago, although it was ruled with uniform line spacings and admittedly suffered from severe levels of stray light.

Type V Holographic Gratings

Holographic recording geometries exist which utilize visible light to generate groove patterns which correct aberrations at shorter wavelengths. Such a geometry, tailored to the proposed varied-space plano gratings, is discussed at length in reference 4. We mention here only the main results:

- (1) Two real point sources (visible wavelength) are placed on a circle centered at the grating to be recorded. As the grating is flat, both sources may be placed on the same side of the grating (e.g., above or below).
- (2) A small change in the radius of this circle allows the corrected wavelength to be tuned over a large range.
- (3) This wavelength-scaling procedure results in a finite aberration at the corrected wavelength, which increases as the square of the grating size. Multi-partite recordings must therefore be used to obtain high resolutions in the EUV or soft X-ray.

Figure 2c shows the ray trace results for one example, where the recording wavelength was assumed to be $\lambda = 3637 \text{ \AA}$ and maximum aberration-correction was chosen at $\lambda = 304 \text{ \AA}$. Five recordings were used across the grating aperture of 180 mm, with the result that aberrations were comparable to the mechanically-ruled straight-groove design of Figure 2a.

This type of holographic grating is designated as a "Type V" variety, being distinguishable from other holographic varieties by its plane surface and its intended use in converging light.

An interesting other application of visible holography is in the potential fabrication of a varied line-space echelle operating in high order. In this case, the recording wavelength scales naturally by the magnitude of the echelle order in which the grating is used, maintaining complete stigmatism. Thus, if an echelle is to operate near 100 \AA in spectral order ~ 60 , visible holography will directly record the stigmatic groove patterns. However, the required groove profiles are triangles at large blaze angles, requiring that special techniques be used in the processing of the photoresist.

Interferometry in the EUV and Soft X-ray

Extreme Ultraviolet

Figure 8 illustrates a new optical system which can be used to measure wavefront aberrations for the proposed varied line-space plano gratings. It takes advantage of the stigmatic zero-order image off of a plane grating in converging light. In essence, the grating is illuminated in reverse, starting with two stigmatic points corresponding to the correction wavelength and to the zero order image. Thus, an aberration-free grating will yield a perfectly spherical wave, which is imaged upon a flat film surface by an off-axis paraboloid. A unique feature to this interferometer is the absence of an exit pinhole. This will greatly increase its sensitivity in this wavelength region, where the required pinhole sizes are very small and where the light sources are inherently weak. Note that the aberrations of the toroidal grating determine the resolution limit of this interferometer. This was minimized by choosing the two source points to lie at the quasi-stigmatic points on either side of the toroidal normal.

To illustrate the diagnostic capabilities of this interferometer, simulations were made of the fringe patterns generated under specified conditions (the aberration contributions of the toroidal grating have not been included). The inset of Figure 8 shows these results. The top panel shows a fringe pattern produced at 304 \AA by a straight groove VLS grating like that designed for the EUVE spectrometer. It illustrates the stigmatism from the in plane grating rays, and increase in aberration off plane. A perfect concentric groove grating produces a perfect image; an interferogram from an imperfect grating with ruling errors that increase off plane has been shown (in the bottom panel) to illustrate the sensitivity of the interferometer. The errors shown result in a resolution of $\sim 10^4$. Thus errors that would degrade the resolution to less than 30,000 would be easily detectable using this method.

Soft X-ray

Figure 9 illustrates a second interferometer which can extend into the soft X-ray, and is based upon similar principles as the above design. A monochromatic light source is placed behind a pinhole which provides diffraction-limited waves emanating at an intersection of two Rowland circles. These Rowland circles correspond to two multi-layered spherical mirrors, which split and focus the incident beam. The spatial separation of the two respective images (A and B) can be selected by choosing the correct separation of the Rowland circle centers (A and B); the light source remains fixed in position during this motion. A small flat mirror near the image A is again employed as with the previous interferometer. In the absence of grating aberrations, a perfectly spherical wavefront should emerge. The aberrant fringe pattern is therefore recorded by using a spherical detector (e.g., film). Alternately, an off-axis camera mirror may be used in combination with a flat detecting surface.

Coherence Lengths

The coherence length required for the light source is small, being equal to the path-length retardation across the grating sample (the aberrant fringe contribution is negligible). For example, using a wavelength of 304 Å and a 100 mm grating with a nominal line-density of 2000 mm⁻¹, the total path-length difference is only 6 mm. This corresponds to a decay time of only $\sim 2 \times 10^{-11}$ seconds for the emission-line of the light source, or a line width of 3 mÅ. Conventional laboratory sources, such as the Penning discharge source,¹³ should be able to achieve this line width when operated at low pressures.

References

1. Kahn, S. M., Seward, S. P., and Chlebowski, F. T., Ap. J., in press (1984).
2. Dupree, A. K., "The astrophysical interest of EUV observations of extra-solar objects," Harvard-Smithsonian Center for Astrophysics, preprint no. 1452.
3. Hettrick, M. C., and Bowyer, S., Appl. Opt., Vol. 22, p. 3921. 1983.
4. Hettrick, M. C., Appl. Opt. Sept. 15, 1984.
5. Hettrick, M. C., and Bowyer, S., "A new class of grazing incidence telescopes for soft X-ray and EUV spectroscopy," accepted in Appl. Opt. (1984).
6. Murty, M. V. R. K., J. Opt. Soc. Am., Vol. 52, p. 768. 1962.
7. Kita, T., Harada, T., Nakano, N., and Kuroda, H., Appl. Opt., Vol. 22, p. 512. 1983.
8. Edelstein, J., Hettrick, M. C., Mrowka, S., Jelinsky, P., and Martin, C., Appl. Opt. Oct. 1, 1984.
9. Bowyer, S., Malina, R., Lampton, M., Finley, D., Paresce, F., and Penegor, G., Proc. Soc. Photo-Opt. Instrum. Eng., Vol. 279, p. 176. 1981.
10. Barbee, T. W., Mrowka, S., and Hettrick, M. C., "Extreme Ultraviolet Measurements of Molybdenum and Silicon," submitted Appl. Opt. (August, 1984).
11. Bunner, A., Perkin-Elmer Corporation, private communication (1984).
12. Sakayanagi, Y., Sci. Light, Vol. 3, p. 1. 1954 (Tokyo).
13. Finley, D. S., Bowyer, S., Paresce, F., and Malina, R. F., Appl. Opt., Vol. 18, p. 649. 1979.

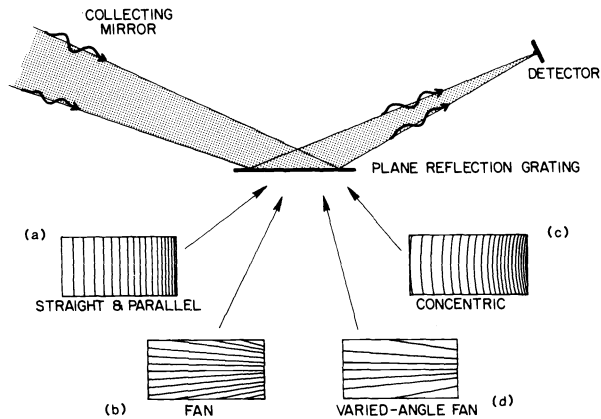


Figure 1. Plane reflection gratings in converging light. Several solutions for the groove spacings are shown.

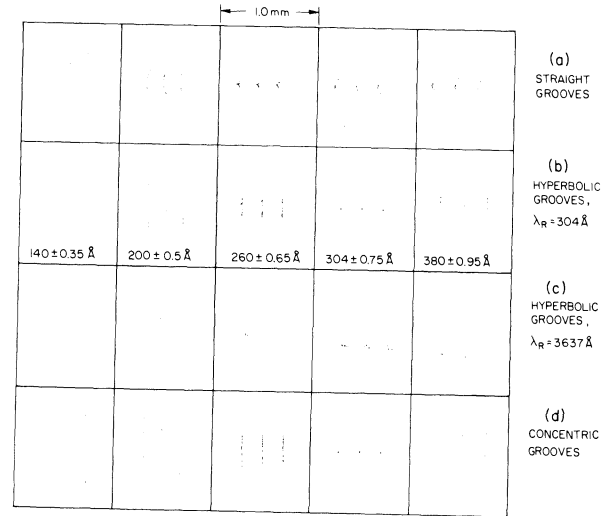


Figure 2. Raytrace spot diagrams for (a) straight grooves, (b) stigmatic hyperbolas, (c) quasi-stigmatic hyperbolas generated by visible holography, and (d) concentric grooves. In all cases, the tangential focal surfaces have been employed, and each wavelength in the triplets is separated by $\Delta\lambda/\lambda = 1/400$.

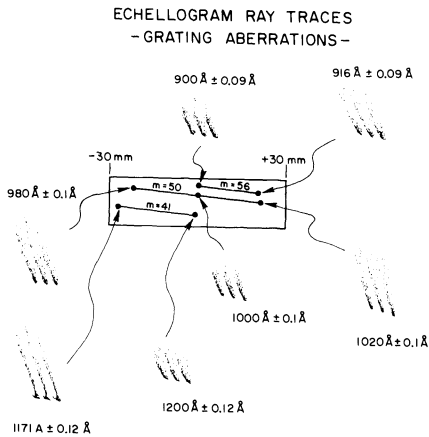


Figure 3. Raytrace results for a two-element echelle spectrometer. A grating resolving power of 40,000 is achieved across the 900-1200 Å bandpass.

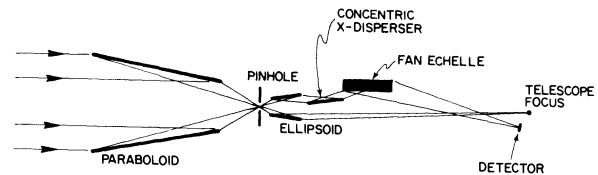


Figure 4. A grazing incidence telescope-spectrometer instrument, consisting of only four grazing reflections. The echelle is a conical diffraction fan grating, and the cross-disperser is a concentric groove grating.

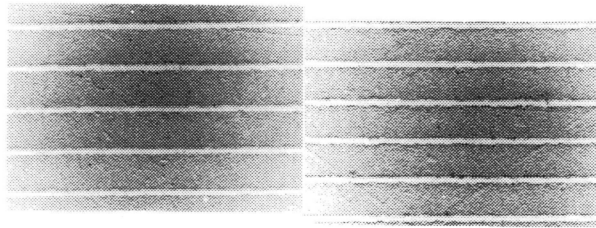


Figure 5. Electron micrographs of Hitachi straight-groove varied line-space plano grating; line density is 1400 l/mm and 1600 l/mm.

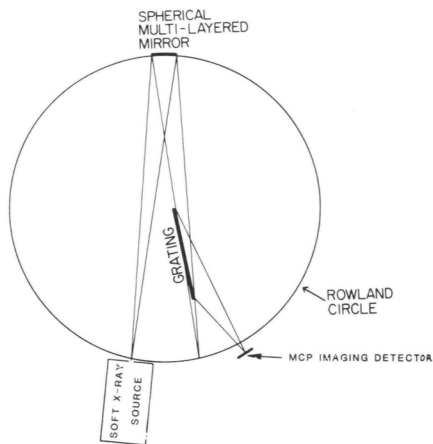


Figure 6. Laboratory apparatus for measuring imaging and scattering performance of plano VLS gratings, to be used for preflight testing of Extreme Ultraviolet Explorer Spectrometer gratings. Spherical mirror may be coated with Osmium ($\lambda > 300 \text{ \AA}$) or multilayers ($\lambda < 300 \text{ \AA}$).

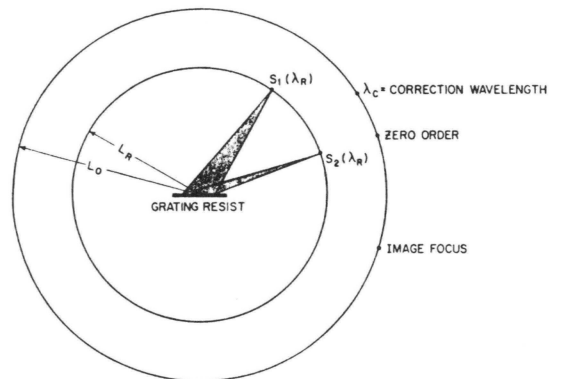


Figure 7. Recording geometry for Type V holographic grating. The outer circle includes the image focus, the zero order image and the correction wavelength λ_C . The inner circle passes through the two recording sources, and the virtual recording source on the opposite side of the grating.

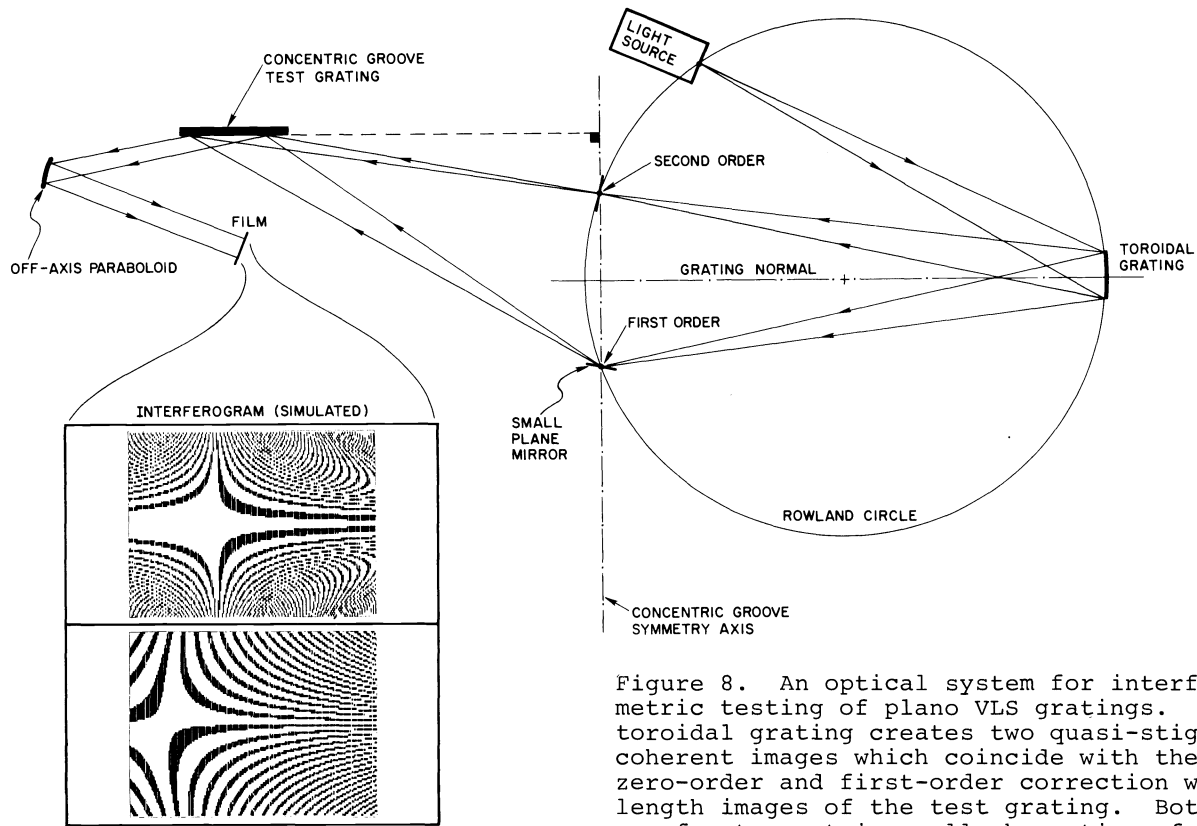


Figure 8. An optical system for interferometric testing of plano VLS gratings. The toroidal grating creates two quasi-stigmatic, coherent images which coincide with the zero-order and first-order correction wavelength images of the test grating. Both wavefronts contain small aberrations from the toroidal grating; the first-order wave front is perturbed in addition by any ruling errors in the test grating. The aberrant wave front diverging from the grating is a record of these ruling errors which can be recorded on film after collimation. The top panel shows the interferogram created by a straight groove plano VLS, while the bottom panel shows that produced by a concentric groove grating with a ruling error that is zero in the figure plane and increases perpendicular to the figure plane. (A perfect CG grating would create no fringes.)

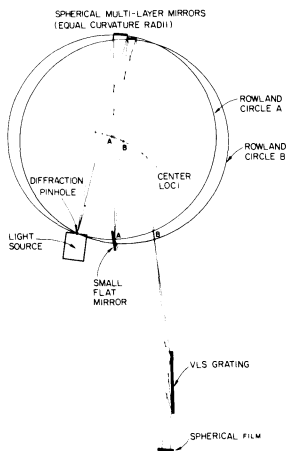


Figure 9. A soft x-ray interferometer, similar in principle to Figure 8, but using 2 spherical multilayer mirrors to split the source light and create 2 point sources.